ADVANCED MATERIALS INTERFACES

www.advmatinterfaces.de

Metal–Organic Framework Coating for the Preservation of Silver Nanowire Surface-Enhanced Raman Scattering Platform

*Hongki Kim, Hyejeong Jang, Jeong Moon, Jihyun Byun, Jinyoung Jeong, Juyeon Jung, Eun-Kyung Lim, and Taejoon Kang**

Ag nanostructures are investigated as efficient plasmonic platforms because of their superior optical properties. However, the easy corrosion of Ag surfaces by reaction with oxygen or sulfur in the atmosphere can seriously affect the optical properties of Ag nanostructures, limiting the stable operation of Ag platforms. Herein, it is reported that a metal–organic framework (MOF) enables an Ag nanowire (NW) surface-enhanced Raman scattering (SERS) platform to be corrosion resistant. A single Ag NW on a film (Ag-NOF), an effective SERS-active platform, is coated with the zeolitic imidazolate framework-8, and then the corrosion resistance of the Ag-NOF structures is examined under a variety of harsh environmental conditions. Interestingly, the MOF-coated Ag-NOF platforms are found to provide excellent oxidation and sulfidation resistance. With the MOF coating, the SERS signals of the Ag-NOF structures are well maintained under harsh conditions, while the signals are reduced without MOF coating. More importantly, it is clearly verified that the MOF coating preserves the DNA sensing performance of the Ag-NOF platform even after storage under several environmental conditions. Based on the results, it is anticipated that these MOF-coated Ag-NOF structures will be used as long-term stable SERS sensors for the detection of biological and chemical molecules.

1. Introduction

Surface-enhanced Raman scattering (SERS) is a fascinating phenomenon that remarkably increases the Raman signals of molecules near noble metallic nanostructures.[1,2] This dramatic signal enhancement allows highly sensitive molecular detection even at the single-molecule level.[3,4] Therefore, SERS has been applied as a powerful analytical technique for the identification of chemical and biological species at trace concentrations.[5] The most frequently used materials in SERS-active platforms are coinage metals such as silver, gold, and copper.[6] Among these metals, the use of Ag is advantageous in the development of SERS-active platforms because of its high interband transition frequency, which enables the production of surface plasmon resonance in the entire visible range, and the large dielectric constant, which can produce strong SERS enhancement.[6–9] Despite these advantages, SERS-active Ag structures often suffer from corrosion by oxygen and sulfur in the ambient atmosphere, limiting the practical use of Ag platforms.[10,11] The corrosion of Ag nanostructures induces a drastic change in or disappearance of the surface plasmon resonance properties originating from free electrons at the Ag surface.[11–13] Since surface plasmons are mainly confined within tens of nanometers, the formation of a thin corrosion layer can seriously affect the optical properties of Ag structures.[13] Another important issue in the development of Ag-based SERS sensing platforms is the poor stability of bioreceptors on the surface of Ag structures. Bioreceptors such as DNA, proteins, and enzymes are sensitive to the ambient atmosphere, temperature, humidity, organic solvents, and so on.[14–16] Therefore, bioreceptors on an Ag surface can easily degrade and lose functionality in the corrosion process. To preserve the sensing ability of Ag SERS sensors, the sensors should be maintained under proper conditions during fabrication, storage, transportation, and handling.[17]

Previously, several approaches have been developed to overcome the poor stability of SERS-active Ag nanostructures by forming protective layers on the Ag surface. For example, core-shell structures, including Ag@TiO_2, Ag@SiO_2, and

Dr. H. Kim, H. Jang, J. Moon, J. Byun, Dr. J. Jung, Dr. E.-K. Lim, Dr. T. Kang
Bionanotechnology Research Center
KRIBB
Daejeon 34141, Korea
E-mail: kangtaejoon@kribb.re.kr

J. Moon
Department of Chemical and Biomolecular Engineering
KAIST
Daejeon 34141, Korea

Dr. J. Jeong
Environmental Disease Research Center
KRIBB
Daejeon 34141, Korea

Dr. J. Jeong, Dr. J. Jung, Dr. E.-K. Lim, Dr. T. Kang
Department of Nanobiotechnology
KRIBB School of Biotechnology
UST
Daejeon 34113, Korea

The ORCID identification number(s) for the author(s) of this article can be found under https://doi.org/10.1002/admi.201900427.

DOI: 10.1002/admi.201900427

Ag@Au, have been developed to improve the chemical stability of Ag nanostructures.[18–21] Al_2O_3 was coated on Ag nanorods by atomic layer deposition technique for suppressing the surface reaction with air.[22] Recently, graphene was employed as a protective layer for Ag nanostructures due to its chemical inertness and impenetrability.[23,24] Although these protection layers prevent the reaction of Ag with oxygen and sulfur, the inevitable Raman signals of these layers may interfere with the accurate analysis of SERS signals.[25–27] Additionally, the protective layer on the plasmonic nanostructures may interrupt the immobilization of biomolecules onto the surfaces of plasmonic nanostructures. The ideal protective layer should be able to be simply coated on an Ag platform and removed without a loss in sensing performance. Furthermore, the layer should prevent the corrosion of Ag nanostructures and preserve the functionality of bioreceptors on the Ag surface in harsh conditions. If the development of this protective layer is feasible, it could widen the practical applicability of Ag SERS platforms in biochemical sensing.

Metal–organic frameworks (MOFs), composed of metal nodes and organic linkers, have been considered promising materials in wide applications such as gas separation, catalysts, drug delivery, and chemical sensing due to their outstanding properties, including high surface area, tunable porosity, organic functionality, stable shelf life, and high thermal stability.[28–32] Recently, Falcaro and Tsung's group reported that the MOF encapsulation of biomolecules is possible under biocompatible conditions, and Singamaneni's group demonstrated that MOFs can be used to preserve the recognition capability of antibodies under harsh conditions.[33–37] Zheng et al. reported the general synthetic method of Metal@MOF hybrid structures and investigated the transport of guest molecules through the MOF by SERS observation.[38] These studies expanded the application areas of MOFs and inspired us to combine an MOF with a SERS-active Ag nanowire (NW) platform. Herein, we report a corrosion-resistant Ag NW SERS platform with an MOF coating. First, it was determined that the zeolitic imidazolate framework-8 (ZIF-8) can be homogeneously grown on a single Ag NW on a film (Ag-NOF) structure and can also be removed after simple washing. We verified that the coating and removal process of MOF does not affect the SERS activity of the Ag-NOF structure. Molecular SERS signals obtained with the Ag-NOF platforms were maintained at more than 95% after the coating and removal of ZIF-8. Second, we demonstrated that the MOF coating can enhance the oxidation and sulfidation resistance of the Ag SERS platform. Only with MOF coating did the Ag-NOF structures provide the 88% retention of SERS signals after storage in harsh conditions (ozone treatment, heating under oxygen flow, and storage for 14 days under ambient conditions). Third, we further showed that the MOF coating enabled the preservation of the sensing performance of the Ag-NOF platform. The prepared Ag-NOF single-stranded DNA (ssDNA) sensors were coated with ZIF-8, treated in several conditions (ozone treatment, heating under oxygen flow, storage for 14 days under ambient conditions, and nuclease treatment), and used for the detection of ssDNA after the removal of ZIF-8. The MOF-coated Ag-NOF sensors successfully detected ssDNA after the harsh treatments, whereas the bare Ag-NOF sensors significantly lost sensing ability after treatment. We expect that the proposed MOF-coated Ag-NOF structures could be stable and efficient biochemical SERS sensing platforms. Furthermore, this method could be applied in the preservation of diverse Ag-based nanostructures in unexpectedly harsh environmental conditions.

2. Results and Discussion

Noble-metal NWs have become promising materials in various research efforts owing to their outstanding physicochemical properties.[39] In particular, the use of single-crystalline noble-metal NWs has received much attention for SERS-based biochemical analyte detection because their well-defined geometries and atomically smooth surfaces provide remarkable reproducibility and signal enhancement.[21,24,40–45] In this regard, we adopted an Ag-NOF architecture as a SERS-active platform. For the fabrication of the Ag-NOF structure, single-crystalline Ag NWs were first synthesized on a sapphire substrate by using the vapor-phase transport method without any surfactant.[40,41] The synthesized Ag NWs had atomically smooth surfaces and diameters of approximately 150 nm. Next, the Ag NWs were transferred onto an Ag film through a lubricant-assisted simple attachment and detachment method.[45] The prepared Ag-NOF sandwich structure provides a line of SERS hot spots along the gap between the NW and film with reliable reproducibility and excellent sensitivity.[40,41] After the construction of Ag-NOF structures, MOF encapsulation was performed to enhance the stability of the Ag platform under various harsh environmental conditions. **Figure 1**a is a schematic illustration of the ZIF-8 coating and removal process on the Ag-NOF structure. For MOF encapsulation, the Ag-NOF platforms were immersed into a ZIF-8 precursor solution that contained 2-methylimidazole and zinc acetate (40:1 molar ratio) for 8 h. During this process, ZIF-8 was nucleated and homogeneously assembled on the Ag-NOF structures. Figure 1b is a scanning electron microscope (SEM) image of the bare Ag-NOF platform, and Figure 1c,d shows SEM images of ZIF-8-coated Ag-NOF structures treated for 20 min and 8 h, respectively. As shown in Figure 1d, thick ZIF-8 layers were formed after reaction for 8 h. We also tried to remove the MOF layers from the Ag-NOF structures and verified that the coated MOF layers can be removed by rinsing with a slightly acidic aqueous solution (Figure S1, Supporting Information).[35–37,46] To optimize the MOF removal buffer, deionized (DI) water and buffers were tested in various pH conditions (Figure S2, Supporting Information). Since ZIF-8 residue increases the pH of aqueous solution, a slightly acidic buffer can dissolve ZIF-8 crystals completely and quickly.[36] We found that phosphate buffer (PB) (pH 5.8) can completely remove ZIF-8 within 5 min; therefore, this removal buffer solution was employed for all experiments. It is important to ensure removal of the ZIF-8 protective coating. If the MOF is not removed, the biorecognition capability of the bioreceptor on Ag surface is degraded and thus target molecules cannot be effectively detected. After the removal of ZIF-8, another SEM image of the Ag-NOF platform was obtained (Figure 1e). In addition, we provided large area SEM images of bare Ag-NOF platforms and those of the same Ag-NOF platforms after coating and removal of MOF

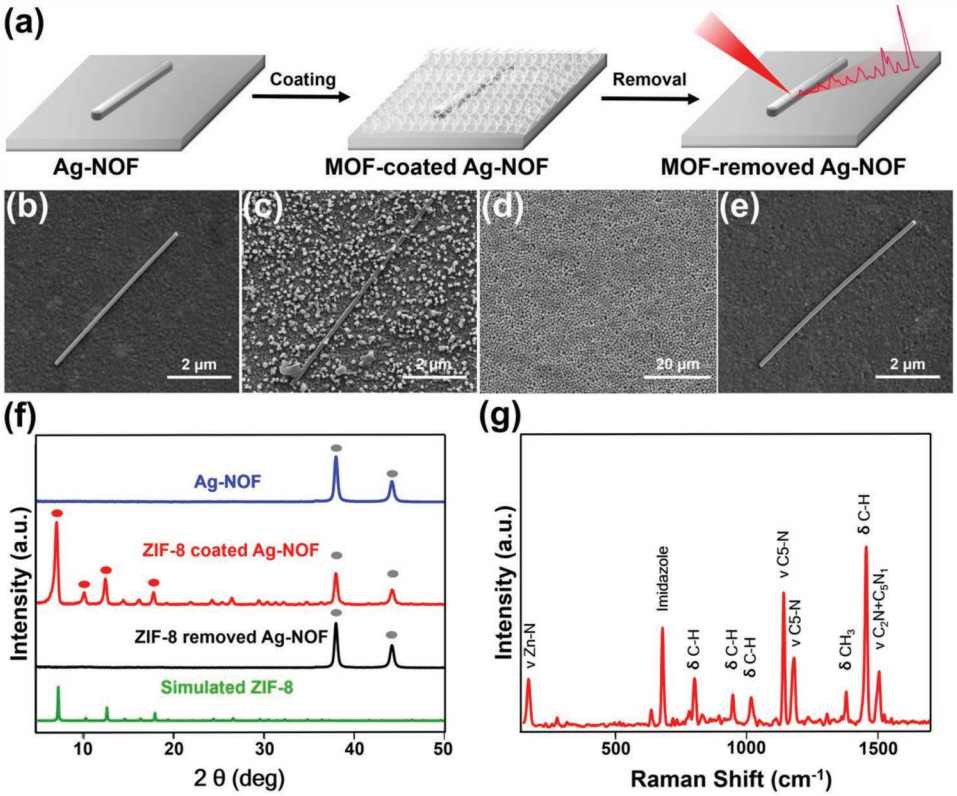

Figure 1. a) Schematic illustration of the MOF coating and removal process on the Ag-NOF platform. b–e) SEM images of the bare Ag-NOF platform before ZIF-8 coating (b), ZIF-8-coated Ag-NOF platform treated for 20 min (c), ZIF-8-coated Ag-NOF platform treated for 8 h (d), and Ag-NOF platform after removal of ZIF-8 (e). f) XRD patterns of the bare Ag-NOF platform (blue), ZIF-8-coated Ag-NOF platform (red), Ag-NOF platform after removal of ZIF-8 (black), and simulated ZIF-8 (green). g) Raman spectra of the ZIF-8-coated Ag-NOF platform.

(Figure S3, Supporting Information).These images clearly shows that the morphology of the Ag-NOF platform is well preserved after the coating and removal of MOF.

To ascertain that ZIF-8 covered the Ag-NOF platform homogeneously, the crystal structure of Ag-NOF was investigated by X-ray diffraction (XRD) before and after the coating of the ZIF-8 layer (Figure 1f). XRD reflection at 38.06° and 44.20°, originating from the (111) and (200) planes of Ag, respectively, were observed only for the bare Ag-NOF structures (blue spectrum in Figure 1f). After coating with ZIF-8, new reflections, marked with red circles, appeared (red spectrum in Figure 1f). These XRD patterns correspond to the simulated ZIF-8 peaks of the (011), (002), (112), and (222) planes (green spectrum in Figure 1f) and agree well with the previously reported literature.[33–37] These results suggest that ZIF-8 was successfully coated on the Ag-NOF platforms. After the simple removal of ZIF-8 with buffer solution, the peaks of ZIF-8 completely disappeared, but the peaks of Ag remained, indicating the complete removal of ZIF-8 (black spectrum in Figure 1f). Additionally, we measured the Raman spectra of ZIF-8-coated Ag-NOF structures (Figure 1g). Strong bands at 168, 686, 1146, and 1458 cm^{-1} were obtained and identified as Zn—N stretching, imidazole ring puckering, C5—N stretching, and methyl bending, respectively.[47] These results indicate that the formation of ZIF-8 crystals on Ag-NOF platforms is highly related to the methyl group and imidazole ring vibration. Fourier transform infrared (FTIR) spectroscopy of ZIF-8 also supports the formation of a ZIF-8 layer on the Ag NW SERS platforms (Figure S4, Supporting Information).[48]

Next, we examined whether the ZIF-8 coating and removal process would compromise the SERS activity of Ag-NOF structures. **Figure 2**a,c,e displays the SERS spectra of brilliant cresyl blue (BCB), benzenethiol (BT), and crystal violet (CV) measured with bare Ag-NOF structures (blue spectra) and with Ag-NOF structures after the coating and removal of MOF (red spectra). All 10 NWs in each structure were randomly selected and measured. The high-quality SERS spectra of BCB, BT, and CV were well preserved after the coating and removal of ZIF-8 on the Ag-NOF platforms. Figure 2b,d,f shows the plots of the representative band intensity of each SERS spectrum (580 cm^{-1} band for BCB, 1572 cm^{-1} band for BT, and 1617 cm^{-1} band for CV) versus the bare and ZIF-8-treated Ag-NOF platforms. Additionally, we measured the SERS signal of molecules from the same position Ag NW before and after the removal of MOF. (Figure S5, Supporting Information). Even after the coating and removal of ZIF-8 layers, the Ag-NOF structures exhibited almost the same SERS activities as those of bare Ag-NOF structures. The representative band intensities of BCB, BT, and CV were retained at 95%, 94%, and 97% after ZIF-8 coating and removal. The small signal difference might be attributed to the remained ZIF-8 which is not completely removed. This observation clearly shows that the ZIF-8 encapsulation and removal

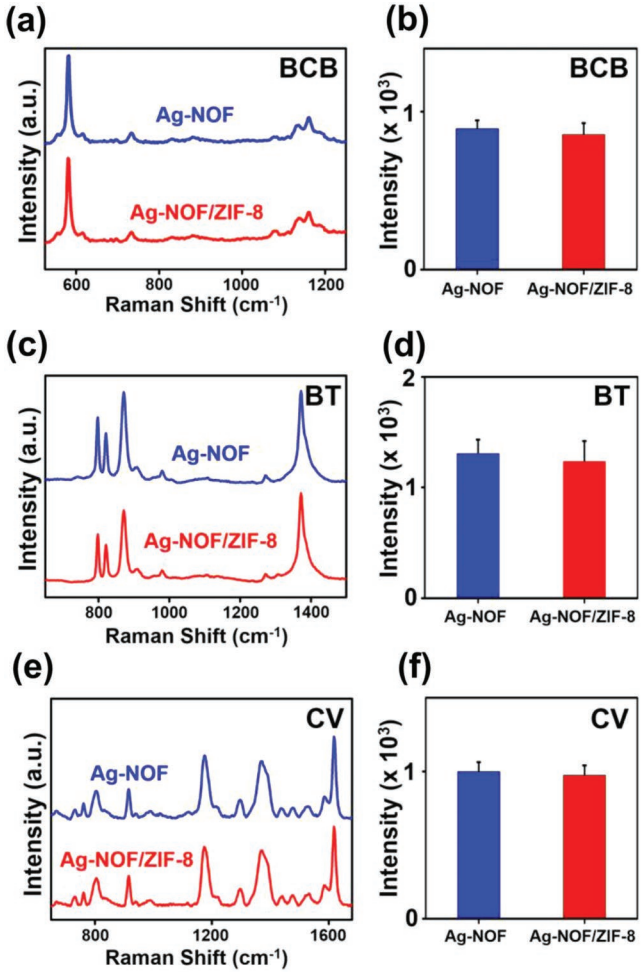

Figure 2. a,c,e) SERS spectra of BCB (a), BT (c), and CV (e) measured with bare Ag-NOF platforms (blue) and with Ag-NOF platforms after the coating and removal of MOF (red). b,d,f) Plots of the representative band intensity of each SERS spectrum (580 cm^{-1} band for BCB, 1572 cm^{-1} band for BT, and 1617 cm^{-1} band for CV) versus the bare (blue) and ZIF-8-treated (red) Ag-NOF platforms. Data represent the mean plus standard deviation from 10 measurements.

process does not negatively affect the SERS performance of the Ag-NOF platforms.

To investigate the resistance of ZIF-8-coated Ag-NOF structures to oxidation and sulfidation, we intentionally exposed the Ag-NOF platforms to various harsh environmental conditions that would commonly result in significant changes in the plasmonic properties of Ag.[10–13] We prepared bare Ag-NOF samples and acquired the SERS signals of BCB immediately after the preparation. We also prepared other Ag-NOF samples, coated the samples with ZIF-8, and stored for 10 min in an ozone generator. After storing, the samples were immersed into removal buffer and SERS signals were obtained. Additionally, we prepared the other Ag-NOF samples, coated the samples with ZIF-8, and stored for 15 min in an ozone generator. After storing and removal of MOF, SERS signals were measured. The tests in the furnace chamber and ambient condition proceeded through the same way above. **Figure 3**a,b shows SERS spectra of BCB obtained with the bare Ag-NOF and ZIF-8-coated Ag-NOF structures, respectively, after ozone treatment. The results clearly show that the SERS enhancement of the bare Ag-NOF platforms almost disappeared, while the strong SERS signals of BCB were maintained with the ZIF-8-coated Ag-NOF structures after ozone treatment (Figure 3b). The results of quantitative band intensity analysis indicate that the MOF coating enabled the preservation of the SERS signals of Ag-NOF platforms at almost 91% (red bars in Figure 3c). Without the MOF coating, the 580 cm^{-1} band intensity of BCB was significantly decreased to ≈20% of the original intensity (blue bars in Figure 3c). Second, we tested the stability of two kinds of Ag-NOF platforms by storing the platforms in a furnace chamber at 95 °C under a 20 sccm flow of O_2 for 0, 8, and 12 h. Figure 3d,e shows the SERS spectra of BCB measured with the bare Ag-NOF and ZIF-8-coated Ag-NOF platforms, respectively, after storage in the furnace chamber. Similar to the ozone treatment results, the SERS signals of the bare Ag-NOF structures were remarkably decreased after storage for 8 and 12 h; however, the signals of the ZIF-8-coated Ag-NOF platforms were maintained regardless of heating and oxygen flow. The plot of the 580 cm^{-1} band intensity versus the treatment time shows that ZIF-8-coated Ag-NOF platforms provided ≈94% of the original SERS intensity and the bare Ag-NOF platforms provided only ≈28% of the original intensity after storage in the furnace chamber (Figure 3f). Finally, we explored the effect of ambient air exposure on the SERS activity of the bare Ag-NOF and ZIF-8-coated Ag-NOF structures. Both platforms were exposed for up to 7 and 14 days in ambient conditions at room temperature. As shown in Figure 3g, the SERS spectra of BCB measured with the bare Ag-NOF platforms decreased as the exposure time increased. The Ag-NOF platforms with MOF coating preserved the SERS signals of BCB after 14 days. Quantitatively, the ZIF-8-coated Ag-NOF structures provided ≈80% of the original intensity, and the bare Ag-NOF showed ≈31% of the original intensity after storage for 14 days (Figure 3i). This result clearly verifies that the MOF coating significantly increased the corrosion resistivity of the Ag-NOF structures.

Additionally, we obtained Ag 3d, O 1s, and S 2p X-ray photoelectron spectroscopy (XPS) spectra of Ag-NOF platforms with or without ZIF-8 coating after storage in harsh conditions (red and blue spectra in **Figure 4**). Before XPS measurements, the MOF-coated Ag-NOF platforms were washed in PB. For comparison, we also measured the XPS spectra of the bare Ag film (black spectra in Figure 4). Figure 4a–c displays the XPS spectra obtained from the Ag-NOF platforms after storage in the ozone generator for 15 min. The bare Ag-NOF platforms showed a shift in the Ag 3d peak of 0.3 eV compared with the peak of metallic Ag (368.1 eV). According to a previous report, the Ag 3d peak can shift to a lower binding energy as the oxidation state of Ag increases.[11,49,50] A shift of 0.3 eV usually corresponds to the formation of Ag_2O. The bare Ag-NOF platforms also showed an O 1s peak at 529.1 eV, indicating the typical O 1s binding energy for Ag_2O. The broad peak at 503.5–532 eV is associated with bulk dissolved oxygen.[49] In contrast, the ZIF-8-coated Ag-NOF structures showed no peak shift compared to those of metallic Ag, suggesting the preservation capability of the MOF coating. S 2p peaks were not observed in either platform because the samples had been stored in the ozone generator. Figure 4d–f shows the XPS spectra measured from

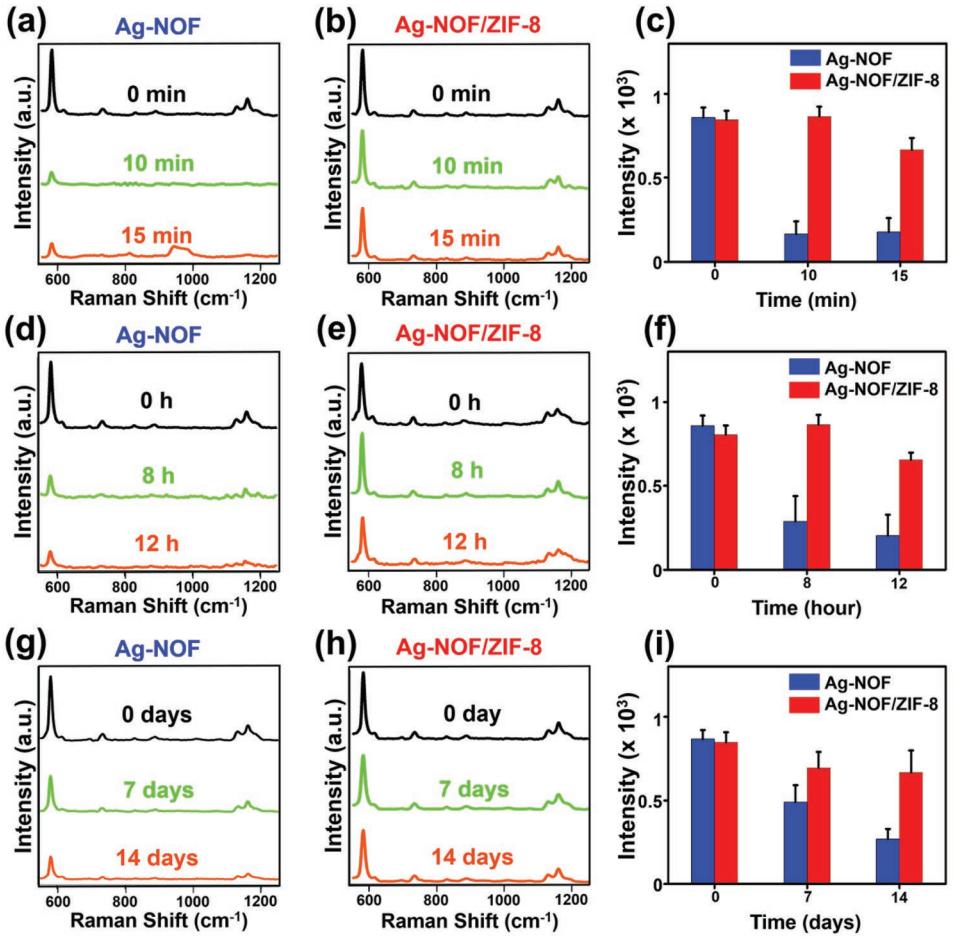

Figure 3. a,b) SERS spectra of BCB measured with bare Ag-NOF platforms (a) and ZIF-8-coated Ag-NOF platforms (b) after storage in an ozone generator for 0, 10, and 15 min. c) Plot of 580 cm^{-1} band intensity versus storage time for Ag-NOF (blue) and ZIF-8-coated Ag-NOF (red) platforms. d,e) SERS spectra of BCB measured with bare Ag-NOF platforms (d) and ZIF-8-coated Ag-NOF platforms (e) after storage in a furnace chamber (20 sccm flow of O_2) for 0, 8, and 12 h. f) Plot of 580 cm^{-1} band intensity versus storage time for Ag-NOF (blue) and ZIF-8-coated Ag-NOF (red) platforms. g,h) SERS spectra of BCB measured with bare Ag-NOF platforms (g) and ZIF-8-coated Ag-NOF platforms (h) after storage under ambient conditions for 0, 7, and 14 days. i) Plot of 580 cm^{-1} band intensity versus storage time for Ag-NOF (blue) and ZIF-8-coated Ag-NOF (red) platforms. After storage of the samples, the bare Ag-NOF platforms were used to measure the SERS spectra of BCB immediately, and the ZIF-8-coated Ag-NOF platforms were washed in PB and used to measure the SERS spectra of BCB. Data represent the mean plus standard deviation from 10 measurements.

two kinds of Ag-NOF platforms after storage in the furnace chamber at 95 °C under a 20 sccm flow of O_2 for 12 h. Similar to the ozone-treated samples, the bare Ag-NOF platforms provided a shifted Ag 3d peak and O 1s peak at 529.1 eV.[11,49,50] Moreover, obtained two peaks at 161 and 163 eV in the S 2p region of the spectra, as shown in Figure 4f. These peaks indicate the formation of Ag_2S and are in good agreement with previous reports.[51,52] After storage in the furnace chamber, the ZIF-8-coated Ag-NOF platforms still did not show a peak shift compared to metallic Ag, confirming the high corrosion resistivity of the MOF coating. Finally, XPS spectra of the bare Ag-NOF and ZIF-8-coated Ag-NOF structures were measured after exposure for 14 days in ambient conditions at room temperature (Figure 4g–i). The bare Ag-NOF structures only showed a shifted Ag 3d peak, an O 1s peak at 529.1 eV, and S 2p peaks at 161 and 163 eV, suggesting the oxidation and sulfidation of the Ag-NOF platforms.[51,52] Considering that the atmospheric corrosion of Ag mainly proceeds toward sulfidation, the strong peaks of Ag_2S are reasonable. From these corrosion resistance experiments under three different harsh conditions, it was proven that the ZIF-8-encapsulated Ag-NOF structures are highly resistant to oxidation and sulfidation; thus, these structures are corrosion-resistant SERS-active platforms. This corrosion resistivity might be due to the molecular sieving effect of ZIF-8 encapsulation. The pore size of ZIF-8 is known as 0.340 nm. Considering the kinetic diameters of oxygen (0.345 nm) and hydrogen sulfur gas (0.360 nm), ZIF-8 can prevent the interaction of gas molecules with the Ag nanostructures.[53–55] When the bare Ag-NOF platforms are exposed to oxygen and sulfur species, these species can easily diffuse to the surface of Ag nanostructures and induce corrosion.[10–13] This phenomenon consequently leads to a decrease in the SERS enhancement of Ag-NOF platforms. Moreover, the coating and removal of ZIF-8 can be performed very easily, and the Ag-NOF platforms can maintain their SERS activity during the coating of MOF, storage in harsh conditions,

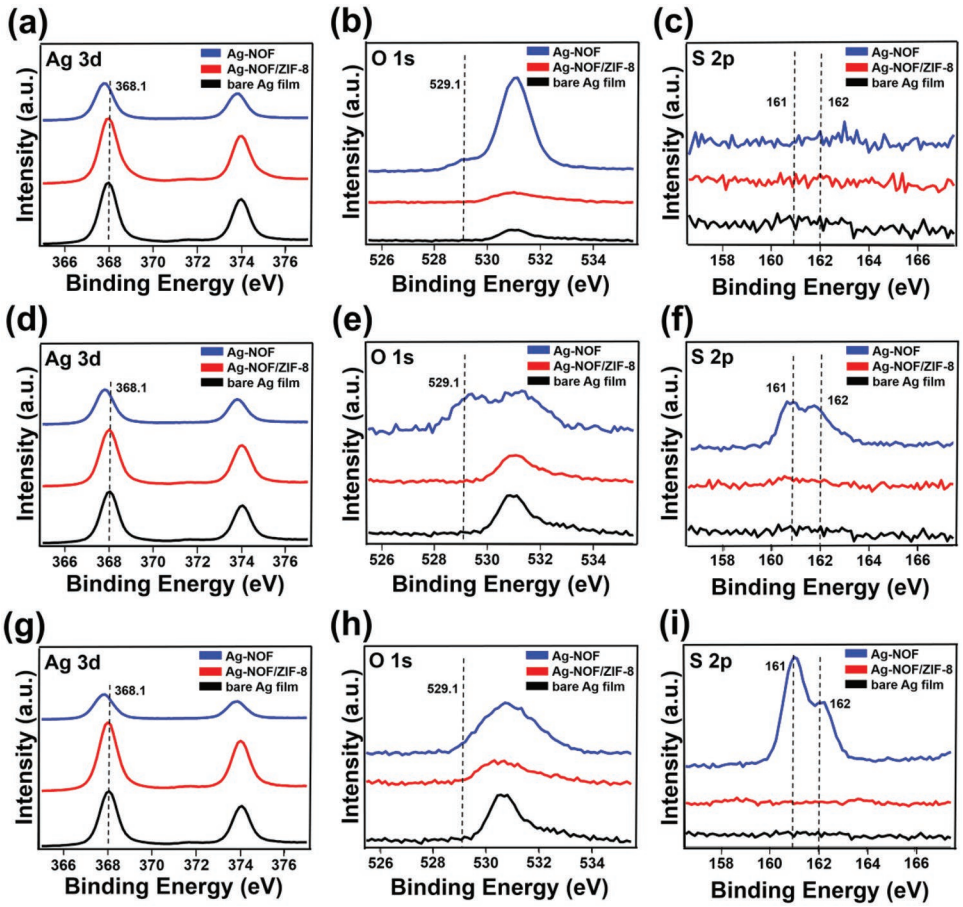

Figure 4. XPS spectra of a) Ag 3d, b) O 1s, and c) S 2p of the bare Ag-NOF platform (blue) and ZIF-8-coated Ag-NOF platform (red) after storage in an ozone generator for 15 min and Ag film (black). XPS spectra of d) Ag 3d, e) O 1s, and f) S 2p of the bare Ag-NOF platform (blue) and ZIF-8-coated Ag-NOF platform (red) after storage in a furnace chamber (20 sccm flow of O_2) for 12 h and Ag film (black). XPS spectra of g) Ag 3d, h) O 1s, and i) S 2p of the bare Ag-NOF platform (blue) and ZIF-8-coated Ag-NOF platform (red) after storage under ambient conditions for 14 days and Ag film (black). After storage of the samples, the bare Ag-NOF platforms were used to measure XPS spectra immediately, and the ZIF-8-coated Ag-NOF platforms were washed in PB and used to measure XPS spectra.

and removal of MOF. In order to fabricate more stable Ag-based SERS biosensor for a longer period of time, it is necessary to study about adjusting the pore size by employing the various types of MOFs.

Single-NOF architectures are stable and efficient SERS-active platforms.[21,24,40–42] Hence, such structures have been employed for the sensitive and accurate detection of nucleic acids and further advanced to sophisticated disease diagnostic sensors.[42–45] The present Ag-NOF structures can also be used for the detection of DNA. Recently, it was reported that MOF coatings can be formed on biological molecules such as proteins, enzymes, and DNA since biomolecules can act as MOF nucleation sites.[33,34] Therefore, we set out to examine the efficiency of ZIF-8-coated Ag-NOF platforms for preserving biosensing ability. **Figure 5**a shows a schematic illustration of the MOF-coated Ag-NOF sensor for the detection of ssDNA after storage in harsh conditions. For the construction of Ag-NOF ssDNA sensors, as-synthesized Ag NWs were modified with thiolated probe DNA and transferred onto an Ag substrate. Next, the Ag-NOF sensors were coated with ZIF-8 and stored in several harsh environmental conditions. In detail, the sensors were stored in an ozone generator for 15 min, in a furnace chamber at 95 °C under 20 sccm flow of O_2 for 12 h, in ambient conditions at room temperature for 2 weeks, or in 1 unit of DNase I for 5 min. DNase I is an endonuclease that nonspecifically cleaves single- and double-stranded DNA.[56] After storage of ZIF-8-coated Ag-NOF sensors, the sensors were washed with PB, incubated with a target DNA (1 nM), and immersed in Cy5-labeled reporter DNA. All DNA sequences are described in Table S1, Supporting Information. For comparison, we performed the same experiments by using the bare Ag-NOF ssDNA sensors without MOF coating. If the Ag-NOF sensors maintain their sensing ability after storage in harsh conditions, a sandwiched probe-target-reporter DNA complex will be formed on the Ag NWs, and thus, strong SERS signals for Cy5 will be obtained. Figure 5b shows the SERS spectra of Cy5 measured with the bare Ag-NOF sensors (blue spectra) and ZIF-8-coated Ag-NOF sensors (red spectra) after harsh treatment and the detection of target ssDNA. Interestingly, we observed strong SERS signals of Cy5 only with the ZIF-8-coated Ag-NOF sensors after the four kinds of treatments. The bare Ag-NOF sensors significantly lost ssDNA sensing ability after

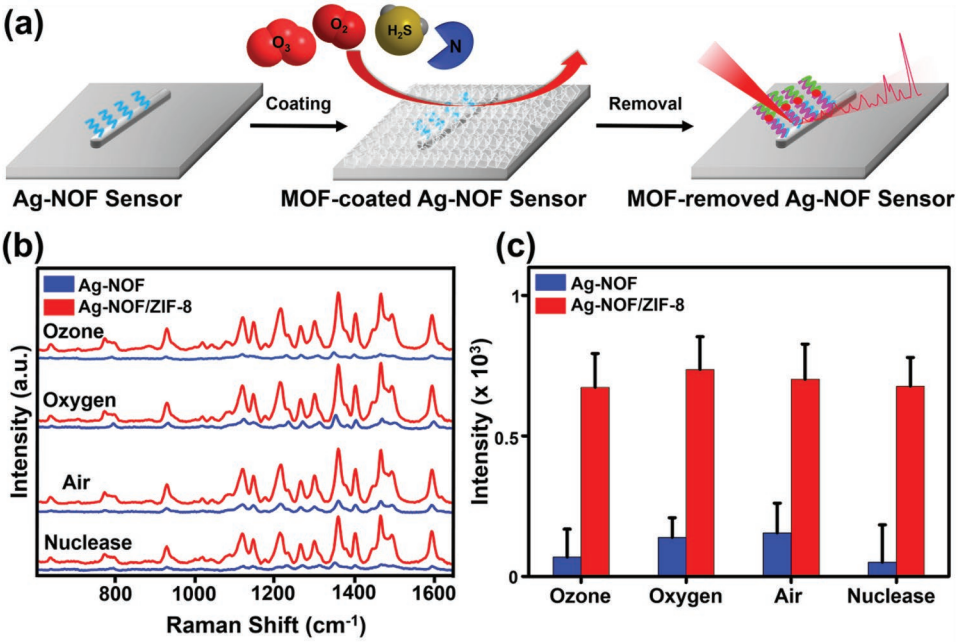

Figure 5. a) Schematic illustration of the Ag-NOF sensor for the detection of ssDNA after storage in harsh conditions. b) SERS spectra of Cy5 measured with bare Ag-NOF (blue) and ZIF-8-coated Ag-NOF sensors (red) after storage in several harsh conditions (ozone generator, oxygen furnace chamber, ambient, and nuclease treatment) and detection of target ssDNA. c) Plot of 1580 cm^{-1} band intensity versus harsh conditions for bare Ag-NOF (blue) and ZIF-8-coated Ag-NOF (red) sensors. After storage of the samples, the bare Ag-NOF sensors were used to detect ssDNA immediately, and the ZIF-8-coated Ag-NOF sensors were washed in PB and used to detect ssDNA. Data represent the mean plus standard deviation from 10 measurements.

treatment. Figure 5c is the plot of the Cy5 1580 cm^{-1} band intensity versus the treatment method, showing the high intensity obtained from the ZIF-8-coated Ag-NOF sensors and the low intensity obtained from the bare Ag-NOF sensors. As shown in the results, the MOF coating effectively prevented the damage of DNA receptors as well as Ag-NOF structures by oxidation, sulfidation, and enzymatic degradation. Considering that the bioreceptors such as DNA and proteins lie in their poor stability at atmosphere, temperature, humidity, organic solvents, and so on, the use of MOF coating is highly advantageous for preserving the sensing capability of biosensors. We expect that the simple MOF coating method will be highly attractive for the practical use of Ag-based biosensing and catalysis fields in unexpected real conditions.[57]

3. Conclusion

We reported a corrosion-resistant Ag-NOF SERS platform with a ZIF-8 coating. MOF encapsulation successfully prevented the oxidation, sulfidation, and enzymatic degradation of Ag NW-based SERS sensors, therefore enabling the preservation of the SERS activity of the Ag nanostructures. We demonstrated the simple coating and removal of MOF on the Ag-NOF platforms and confirmed that SERS signals of molecules could be maintained after the coating and removal of MOF. Furthermore, the ZIF-8-coated Ag-NOF structures exhibited excellent corrosion resistance toward diverse harsh environmental conditions. XPS analysis also supported the corrosion resistance of the ZIF-8-coated Ag-NOF platforms. More importantly, we could detect ssDNA by using the MOF-coated Ag-NOF SERS sensors after storage in an ozone generator, furnace chamber, ambient air, and nuclease solution. This result indicates that the MOF-coated Ag-NOF platforms can be employed as long-term stable SERS sensors. We anticipate that the MOF-encapsulated Ag nanostructures will bring us one step closer to the practical application of Ag-based plasmonic nanostructures in a variety of research fields.

4. Experimental Section

Materials: Ag grain (99.99% purity, 1–3 mm) was purchased from Kojundo Chemical Lab. Co., Ltd (Saitama, Japan). 2-Methylimidazole, zinc acetate dihydrate, sodium phosphate monobasic, sodium phosphate dibasic, BCB, BT, CV, sodium dodecyl sulfate (SDS), formamide solution, and dithiothreitol were purchased from Sigma-Aldrich. Phosphate buffered saline (PBS) and Tween 20 were purchased from Gibco. A NAP-5 column was purchased from GE Healthcare. Ethylenediaminetetraacetic acid (EDTA) and SSPE buffer (0.9 M NaCl, 10 mM $NaH_2PO_4 \cdot H_2O$, 1 mM EDTA, pH 7.4) were purchased from DYNE BIO (Sungnam, Korea). Ethyl alcohol (99.9%) was purchased from Samchun Chemical (Seoul, Korea). DNase I (RNase-free) was obtained from Takara Korea Biomedical Inc. All DNA oligonucleotides were purchased from Bioneer (Daejeon, Korea).

Preparation of Ag-NOF Platforms: Ag NWs were synthesized on a sapphire substrate in a horizontal quartz tube furnace system.[40,41] First, Ag grains were placed in an alumina boat in the middle of the horizontal quartz tube furnace system. Next, the system was heated to 840 °C under an Ar gas flow of 100 sccm. The chamber pressure was maintained at 10 Torr. The Ag NWs were grown approximately 7 cm downstream from the precursor on a sapphire substrate after reaction for 90 min. For the construction of Ag-NOF structures, the as-synthesized Ag NWs were transferred onto an Ag film by using a lubricant (distilled water)-assisted transfer method.[45] The Ag film was prepared on precleaned Si substrates by e-beam-assisted deposition of 10 nm of Cr followed by 300 nm of Ag.

ZIF-8 Coating and Removal on Ag-NOF Platforms: To form ZIF-8 nanostructures on the Ag-NOF platforms, 2-methylimidazole and zinc acetate dihydrate (40:1 molar ratio) were mixed in ultrapure water and quickly aged for 10 s. Then, the Ag-NOF platforms were incubated in a ZIF-8 precursor solution for 4 h and dried by N_2 gas flow. This procedure was repeated to obtain thick ZIF-8 films on the Ag-NOF platforms. For the removal of ZIF-8, the samples were gently rinsed by using 0.5 M PB (pH 5.8) for 5 min.

SERS Measurements with Ag-NOF Platforms: To obtain the SERS spectra of BT, the Ag-NOF platforms were incubated in an ethanolic solution of BT (1 mM) for 12 h, washed with ethanol, and purged with N_2. To obtain the SERS spectra of BCB, a 1 μM ethanolic solution of BCB was incubated on Ag-NOF structures for 15 min. To obtain the SERS spectra of CV, a 1 μM ethanolic solution of CV was incubated on Ag-NOF structures for 15 min.

Storage of Ag-NOF Platforms in Harsh Conditions: First, the bare Ag-NOF and ZIF-8-coated Ag-NOF platforms were stored in an ozone generator (Uvc-750, Omniscience Korea) with an ozone generation rate of 4 g h^{-1}. Second, the two Ag-NOF platforms were placed in the middle of a 1-inch diameter horizontal quartz tube furnace system, and the system was heated to 95 °C under an O_2 gas flow of 20 sccm. Third, the two Ag-NOF platforms were stored in ambient conditions at room temperature. After storage in harsh conditions, the bare Ag-NOF platforms were immediately used for SERS measurements, and the ZIF-8-coated Ag-NOF platforms were washed with PB and used for SERS measurements.

Detection of ssDNA by Using an Ag-NOF Sensor: The as-synthesized Ag NWs were incubated with 5 μM purified probe DNA in 1 M KH_2PO_4 buffer (pH 6.75) for 12 h. Excess probe DNA was washed off with 2 × SSPE (0.9 M NaCl, 10 mM $NaH_2PO_4{\cdot}H_2O$, 1 mM EDTA, pH 7.4) and 0.1% (w/v) SDS solution. The probe DNA-functionalized Ag NWs were transferred to Ag films by using a lubricant (distilled water)-assisted transfer method. Next, the Ag-NOF sensors were coated with ZIF-8 and stored in harsh conditions as described above. In the case of the nuclease treatment, the Ag-NOF sensors were incubated with 1 unit of DNase I in 10 × DNase I reaction buffer (Tris-HCl, 2.5 mM $MgCl_2$, and 0.5 mM $CaCl_2$ at pH 7.6) for 5 min and sequentially immersed into 5 μL of 0.5 M EDTA solution at 80 °C for 2 min to stop the nuclease reaction. Finally, the Ag-NOF sensors were washed twice with ultrapure water. After storage of the Ag-NOF sensors in harsh conditions, the ZIF-8-coated Ag-NOF sensors were washed with PB (pH 5.8) for 5 min. Then, the ZIF-8-removed Ag-NOF sensors were incubated with 1 nM of target ssDNA in hybridization buffer (5 × SSPE, 20% (v/v) formamide solution, and 0.1% (w/v) SDS) for 6 h. After hybridization of target ssDNA, the Ag-NOF sensors were washed with a solution of 2 × SSPE and 0.1% (w/v) SDS. Subsequently, these sensors were incubated with 1 nM of Cy5-labeled reporter DNA in hybridization buffer for 6 h. Finally, the Ag-NOF sensors were sequentially washed with PBST (PBS with 0.05% Tween 20), 0.1 × PBS, and ultrapure water, dried under N_2 stream, and measured by a micro Raman system.

Instrumentation: The morphology of the Ag-NOF and ZIF-8-coated Ag-NOF structures was analyzed by SEM (SEM, Quanta 250 FEG, FEI, Hillsboro, OR, USA) with an acceleration voltage of 10 kV after applying an Au coating. XRD measurements of the samples were recorded on a multipurpose thin-film X-ray diffractometer (RIGAKU) using Cu Kα radiation (1.5406 Å). SERS spectra were obtained using a Raman spectrometer (XperRam 200, Nanobase Inc., Korea). A 632 nm visible diode-pumped solid-state laser with a power of 4 mW was focused on the samples with a beam diameter of 2.5 μm. FTIR measurements were obtained using a Nicolet iS50 spectrometer (Thermo Fisher Scientific Instrument). XPS analyses were carried out using a PHI 5000 VersaProbe (ULVAC-PHI, Osaka, Japan) with a monochromatic Al Kα (1486.6 eV) radiation source.

Supporting Information

Supporting Information is available from the Wiley Online Library or from the author.

Acknowledgements

This research was supported by the Center for BioNano Health-Guard funded by the Ministry of Science and ICT (MSIT) of Korea as Global Frontier Project (H-GUARD_2013M3A6B2078950 and H-GUARD_2014M3A6B2060507), the Bio & Medical Technology Development Program of the National Research Foundation (NRF) funded by MSIT of Korea (NRF-2018M3A9E2022821), the Basic Science Research Program of the NRF funded by MSIT (NRF-2018R1C1B6005424, NRF-2019R1C1C1006867, and NRF-2019R1C1C1006084), the First-Mover Program for Accelerating Disruptive Technology Development through the NRF funded by MSIT of Korea (NRF-2018M3C1B9069834), and KRIBB Research Initiative Program.

Conflict of Interest

The authors declare no conflict of interest.

Keywords

corrosion-resistant, metal–organic frameworks, nanowires, silver, surface-enhanced Raman scattering

Received: March 8, 2019
Revised: April 18, 2019
Published online: May 17, 2019

[1] D. L. Jeanmaire, R. P. V. Duyne, *J. Electroanal. Chem. Interfacial Electrochem.* **1977**, *84*, 1.
[2] M. Moskovits, *Rev. Mod. Phys.* **1985**, *57*, 783.
[3] K. Kneipp, Y. Wang, H. Kneipp, L. T. Perelman, I. Itzkan, R. R. Dasari, M. S. Feld, *Phys. Rev. Lett.* **1997**, *78*, 1667.
[4] S. M. Nie, S. R. Emery, *Science* **1997**, *275*, 1102.
[5] C. Zong, M. Xu, L. J. Xu, T. Wei, X. Ma, X. S. Zheng, R. Hu, B. Ren, *Chem. Rev.* **2018**, *118*, 4946.
[6] B. Sharma, R. R. Frontiera, A.-I. Henry, E. Ringe, R. P. Van Duyne, *Mater. Today* **2012**, *15*, 16.
[7] P. R. West, S. Ishii, G. V. Naik, N. K. Emani, V. M. Shalaev, A. Boltasseva, *Laser Photonics Rev.* **2010**, *4*, 795.
[8] K. C. See, J. B. Spicer, J. Brupbacher, D. Zhang, T. G. Vargo, *J. Phys. Chem. B* **2005**, *109*, 2693.
[9] G. Niaura, G. K. Adolfas, V. L. Vincent, *J. Phys. Chem. B* **1997**, *101*, 9250.
[10] A. Matikainen, T. Nuutinen, T. Itkonen, S. Heinilehto, J. Puustinen, J. Hiltunen, J. Lappalainen, P. Karioja, P. Vahimaa, *Sci. Rep.* **2016**, *6*, 37192.
[11] Y. Han, R. Lupitskyy, T. M. Chou, C. M. Stafford, H. Du, S. Sukhishvili, *Anal. Chem.* **2011**, *83*, 5873.
[12] J. C. Reed, H. Zhu, A. Y. Zhu, C. Li, E. Cubukcu, *Nano Lett.* **2012**, *12*, 4090.
[13] P. Nagpal, N. C. Lindquist, S. H. Oh, D. J. Norris, *Science* **2009**, *325*, 594.
[14] A. S. Schrohl, S. Wurtz, E. Kohn, R. E. Banks, H. J. Nielsen, F. C. Sweep, N. Brunner, *Mol. Cell. Proteomics* **2008**, *7*, 2061.
[15] S. Mitragotri, P. A. Burke, R. Langer, *Nat. Rev. Drug Discovery* **2014**, *13*, 655.
[16] N. Savage, *Nature* **2014**, *507*, S8.
[17] J. Zhang, E. Pritchard, X. Hu, T. Valentin, B. Panilaitis, F. G. Omenetto, D. L. Kaplan, *Proc. Natl. Acad. Sci. USA* **2012**, *109*, 11981.
[18] T. Hirakawa, P. V. Kamat, *J. Am. Chem. Soc.* **2005**, *127*, 3928.

[19] J. F. Li, Y. F. Huang, Y. Ding, Z. L. Yang, S. B. Li, X. S. Zhou, F. R. Fan, W. Zhang, Z. Y. Zhou, D. Y. Wu, B. Ren, Z. L. Wang, Z. Q. Tian, *Nature* **2010**, *464*, 392.
[20] C. Gao, Z. Lu, Y. Liu, Q. Zhang, M. Chi, Q. Cheng, Y. Yin, *Angew. Chem., Int. Ed.* **2012**, *51*, 5629.
[21] H. Lee, Y. Yoo, T. Kang, J. In, M. K. Seo, B. Kim, *Small* **2012**, *8*, 1527.
[22] L. Ma, Y. Huang, M. Hou, Z. Xie, Z. Zhang, *Sci. Rep.* **2015**, *5*, 12890.
[23] M. Losurdo, I. Bergmair, B. Dastmalchi, T. H. Kim, M. M. Giangregroio, W. Y. Jiao, G. V. Bianco, A. S. Brown, K. Hingerl, G. Bruno, *Adv. Funct. Mater.* **2014**, *24*, 1864.
[24] H. Kim, M. L. Seol, D. I. Lee, J. Lee, I. S. Kang, H. Lee, T. Kang, Y. K. Choi, B. Kim, *Nanoscale* **2016**, *8*, 8878.
[25] J. F. John, S. Mahurin, S. Dai, M. J. Sepaniak, *J. Raman Spectrosc.* **2010**, *41*, 4.
[26] X. Zhang, J. Zhao, A. V. Whitney, J. W. Elam, R. P. Van Duyne, *J. Am. Chem. Soc.* **2006**, *128*, 10304.
[27] Y. Zhu, X. Jiang, H. Wang, S. Wang, H. Wang, B. Sun, Y. Su, Y. He, *Anal. Chem.* **2015**, *87*, 6631.
[28] O. M. Yaghi, M. O'Keeffe, N. W. Ockwig, H. K. Chae, M. Eddaoudi, J. Kim, *Nature* **2003**, *423*, 705.
[29] H. Zhu, X. Yang, E. D. Cranston, S. Zhu, *Adv. Mater.* **2016**, *28*, 7652.
[30] Y. Liu, W. Xuan, Y. Cui, *Adv. Mater.* **2010**, *22*, 4112.
[31] P. Horcajada, C. Serre, M. Vallet-Regi, M. Sebban, F. Taulelle, G. Ferey, *Angew. Chem., Int. Ed.* **2006**, *45*, 5974.
[32] L. E. Kreno, K. Leong, O. K. Farha, M. Allendorf, R. P. Van Duyne, J. T. Hupp, *Chem. Rev.* **2012**, *112*, 1105.
[33] K. Liang, R. Ricco, C. M. Doherty, M. J. Styles, S. Bell, N. Kirby, S. Mudie, D. Haylock, A. J. Hill, C. J. Doonan, P. Falcaro, *Nat. Commun.* **2015**, *6*, 7240.
[34] F. K. Shieh, S. C. Wang, C. I. Yen, C. C. Wu, S. Dutta, L. Y. Chou, J. V. Morabito, P. Hu, M. H. Hsu, K. C. Wu, C. K. Tsung, *J. Am. Chem. Soc.* **2015**, *137*, 4276.
[35] C. Wang, S. Tadepalli, J. Luan, K. K. Liu, J. J. Morrissey, E. D. Kharasch, R. R. Naik, S. Singamaneni, *Adv. Mater.* **2017**, *29*, 1604433.
[36] C. Wang, H. Sun, J. Luan, Q. Jiang, S. Tadepalli, J. J. Morrissey, E. D. Kharasch, S. Singamaneni, *Chem. Mater.* **2018**, *30*, 1291.
[37] C. Wang, L. Wang, S. Tadepalli, J. J. Morrissey, E. D. Kharasch, R. R. Naik, S. Singamaneni, *ACS Sens.* **2018**, *3*, 342.
[38] G. Zheng, S. de Marchi, V. López-Puente, K. Sentosun, L. Polavarapu, I. Pérez-Juste, E. H. Hill, S. Bals, L. M. Liz-Marzán, I. Pastoriza-Santos, J. Pérez-Juste, *Small* **2016**, *12*, 3935.
[39] Z. Y. Fan, J. C. Ho, T. Takahashi, R. Yerushalmi, K. Takei, A. C. Ford, Y. L. Chueh, A. Javey, *Adv. Mater.* **2009**, *21*, 3730.
[40] I. Yoon, T. Kang, W. Choi, J. Kim, Y. Yoo, S.-W. Joo, Q.-H. Park, H. Ihee, B. Kim, *J. Am. Chem. Soc.* **2009**, *131*, 758.
[41] P. Mohanty, I. Yoon, T. Kang, K. Seo, K. S. K. Varadwaj, W. Choi, Q.-H. Park, J. P. Ahn, Y. D. Suh, H. Ihee, B. Kim, *J. Am. Chem. Soc.* **2007**, *129*, 9576.
[42] G. Eom, H. Kim, A. Hwang, J. Moon, H.-Y. Son, Y. Choi, J. Moon, D. Kim, M. Lee, E.-K. Lim, J. Jeong, Y.-M. Huh, M.-K. Seo, T. Kang, B. Kim, *Adv. Funct. Mater.* **2017**, *27*, 1701832.
[43] R. Gwak, H. Kim, S. M. Yoo, S. Y. Lee, G.-J. Lee, M.-K. Lee, C.-K. Rhee, T. Kang, B. Kim, *Sci. Rep.* **2016**, *6*, 19646.
[44] T. Kang, H. Kim, J. M. Lee, H. Lee, Y.-S. Choi, G. Kang, M.-K. Seo, B. H. Chung, Y. Jung, B. Kim, *Small* **2014**, *10*, 3795.
[45] H. Kim, T. Kang, H. Lee, H. Ryoo, S. M. Yoo, S. Y. Lee, B. Kim, *Chem. - Asian J.* **2013**, *8*, 3010.
[46] H. Zheng, Y. Zhang, L. Liu, W. Wan, P. Guo, A. M. Nystrom, X. Zou, *J. Am. Chem. Soc.* **2016**, *138*, 962.
[47] G. Kumari, K. Jayaramulu, T. K. Maji, C. Narayana, *J. Phys. Chem. A* **2013**, *117*, 11006.
[48] Y. Hu, H. Kazemian, S. Rohani, Y. Huang, Y. Song, *Chem. Commun.* **2011**, *47*, 12694.
[49] G. I. N. Waterhouse, G. A. Bowmaker, J. B. Metson, *Appl. Surf. Sci.* **2001**, *183*, 191.
[50] D. C. Choo, T. W. Kim, *Sci. Rep.* **2017**, *7*, 1696.
[51] J. L. Elechiguerra, L. Larios-Lopez, C. Liu, D. Garcia-Gutierrez, A. Camacho-Bragado, M. J. Yacaman, *Chem. Mater.* **2005**, *17*, 6042.
[52] Y. Wan, X. Wang, X. Wang, Y. Li, H. Sun, K. Zhang, *Int. J. Electrochem. Sci.* **2015**, *10*, 2336.
[53] H. Bux, F. Liang, Y. Li, J. Cravillon, M. Wiebcke, J. Caro, *J. Am. Chem. Soc.* **2009**, *131*, 16000.
[54] W. T. Koo, S. Qiao, A. F. Ogata, G. Jha, J. S. Jang, V. T. Chen, I. D. Kim, R. M. Penner, *ACS Nano* **2017**, *11*, 9276.
[55] J. Lee, O. K. Farha, J. Roberts, K. A. Scheidt, S. T. Nguyen, J. T. Hupp, *Chem. Soc. Rev.* **2009**, *38*, 1450.
[56] K. J. Lee, W. S. Lee, A. Hwang, J. Moon, T. Kang, K. Park, J. Jeong, *Analyst* **2018**, *143*, 332.
[57] S. Rodal-Cedeira, V. Montes-García, L. Polavarapu, D. M. Solís, H. Heidari, A. L. Porta, M. Angiola, A. Martucci, J. M. Taboada, F. Obelleiro, S. Bals, J. Pérez-Juste, I. Pastoriza-Santos, *Chem. Mater.* **2016**, *28*, 9169.

